



Contents lists available at ScienceDirect



Catalysis Today

journal homepage: www.elsevier.com/locate/cattod

Acceptorless dehydrogenation of *N*-heterocycles by supported Pt catalysts

Sondomoyee K. Moromi^a, S.M.A. H. Siddiki^b, Kenichi Kon^{a,b}, Takashi Toyao^{a,b}, Ken-ichi Shimizu^{a,b,*}

^a Institute for Catalysis, Hokkaido University, N-21, W-10, Sapporo 001-0021, Japan

^b Elements Strategy Initiative for Catalysts and Batteries, Kyoto University, Katsura, Kyoto 615-8520, Japan

ARTICLE INFO

Article history:

Received 12 January 2016

Received in revised form 2 June 2016

Accepted 10 June 2016

Available online xxxx

Keywords:

Pt nanoparticles

Dehydrogenation

N-heterocycles

Hydrogen storage

ABSTRACT

Pt metal nanoparticles loaded on various supports and carbon-supported various metal catalysts are tested for dehydrogenation of 6-methyl-1,2,3,4-tetrahydroquinoline to 6-methyl-quinoline under oxidant-free conditions. In the 20 types of the catalysts screened, carbon-supported Pt catalyst (Pt/C) shows the highest activity. Pt/C is reusable after the reaction and is effective for dehydrogenation of various *N*-heterocycles (tetrahydroquinolines and indoline). Pt/C is also effective for hydrogenation of quinoline under 3 bar H₂. The results demonstrate that this catalytic method may be useful for an organic hidride-based hydrogen storage system.

© 2016 Elsevier B.V. All rights reserved.

1. Introduction

Catalytic dehydrogenation [1–9] and oxidation [10–21] of saturated *N*-heterocycles are of fundamental importance in the synthesis of nitrogen-containing aromatics. Previous methods [10–21] are based on the catalytic oxidation of *N*-heterocycles using an external oxidant such as O₂ and stoichiometric oxidants, but use of the oxidant potentially limits selectivity and functional group tolerance. An alternative method is the catalytic dehydrogenation of *N*-heterocycles in the absence of oxidants [1–9]. Recently reported homogeneous catalytic methods with Ir [4,5,7], Ru [8], Co [6] and Fe [9] catalysts were effective for the reaction, but most of these methods have drawbacks such as low turnover number (TON) and difficulties in catalyst/product separation and reuse of the homogeneous catalyst [5–9]. A few reports showed acceptorless dehydrogenation of *N*-heterocycles with heterogeneous catalysts [1–3]. For example, Kaneda et al. developed Pd [1] and Cu catalysts [2] for dehydrogenation of indolines and tetrahydroquinoline, respectively. For a model dehydrogenation of 1,2,3,4-tetrahydroquinoline, the previous homogeneous [4,7,8,6,9] and heterogeneous [2,3] catalysts showed limited TON in a range of 3.3–87. Among these examples, a few studies have suc-

ceeded in the reversible dehydrogenation-hydrogenation reactions of *N*-heterocycles with a single catalyst [2,4–6,9]. This reversible transformation is of particular importance from a viewpoint of organic hydrides for hydrogen storage system. As a part of our continuous studies in heterogeneous catalysis for oxidant-free dehydrogenation reactions [22], we report herein dehydrogenation of saturated *N*-heterocycles by a Pt/C catalyst, which shows higher TON for dehydrogenation of tetrahydroquinoline than previous catalytic systems. Additionally, Pt/C is effective for the reverse reaction, that is hydrogenation of quinoline into tetrahydroquinoline under 3 bar H₂.

2. Experimental

2.1. Catalyst preparation

Commercially available organic and inorganic compounds (Tokyo Chemical Industry, Kanto Chemical) were used without further purification. The standard carbon support, Vulcan XC72 (210 m² g⁻¹), was commercially supplied. γ-Al₂O₃ (124 m² g⁻¹) was prepared by calcination of γ-AlOOH (Catapal B Alumina from Sasol) at 900 °C for 3 h. SiO₂ (Q-10, 300 m² g⁻¹) was supplied from Fuji Silysia Chemical Ltd. TiO₂ (JRC-TIO-4, 50 m² g⁻¹), MgO (JRC-MGO-3, 19 m² g⁻¹), SiO₂-Al₂O₃ (JRC-SAL-2, Al₂O₃ = 13.75 wt%, 560 m² g⁻¹) and HBEA zeolite (SiO₂/Al₂O₃ = 25 ± 5, JRC-Z-HB25) were supplied from Catalysis Society of Japan. Nb₂O₅ (54 m² g⁻¹), ZrO₂ and SnO₂ were prepared by calcination of Nb₂O₅·nH₂O

* Corresponding author at: Institute for Catalysis, Hokkaido University, N-21, W-10, Sapporo 001-0021, Japan.

E-mail address: kshimizu@cat.hokudai.ac.jp (K.-i. Shimizu).

(CBMM), $\text{ZrO}_2 \cdot n\text{H}_2\text{O}$ and H_2SnO_3 (Kojundo Chemical Laboratory Co., Ltd.), respectively, at 500°C for 3 h.

A precursor of the 5 wt% Pt/C catalyst was prepared by impregnation method; a mixture of carbon (Vulcan XC72) and aqueous HNO_3 solution of $\text{Pt}(\text{NH}_3)_2(\text{NO}_3)_2$ (Furuya Metal Co., Ltd.) was evaporated at 50°C , followed by drying at 90°C for 12 h. The reduced Pt/C catalyst, designated as Pt/C, was prepared by reduction of the precursor ($\text{Pt}(\text{NH}_3)_2(\text{NO}_3)_2$ -loaded carbon) in a pyrex tube under H_2 flow ($20\text{ cm}^3\text{ min}^{-1}$) at 300°C for 0.5 h. The other Pt catalysts were prepared by the same method as Pt/C. Carbon-supported metal catalysts, designated as M/C (M = Rh, Pd, Ir, Ru, Ni, Cu, Co, Ag), with metal loading of 5 wt% were prepared by impregnation method by the similar manner as Pt/C using aqueous solution of metal nitrates (for Ni, Cu, Co, Ag) or $\text{IrCl}_3 \cdot n\text{H}_2\text{O}$ or aqueous HNO_3 solution of $\text{Rh}(\text{NO}_3)_3$ (Furuya Metal Co., Ltd.) or Pd ($\text{NH}_3)_2(\text{NO}_3)_2$ (Kojima Chemicals Co., Ltd.). These catalysts were reduced under H_2 flow at 300°C for 0.5 h. Platinum oxides-loaded carbon (PtOx/C) was prepared by calcination of the $\text{Pt}(\text{NH}_3)_2(\text{NO}_3)_2$ -loaded C in air at 300°C for 0.5 h.

2.2. Catalyst characterization

Temperature programmed reduction by H_2 ($\text{H}_2\text{-TPR}$) was carried out by BELCAT (MicrotracBEL). PtOx/C (20 mg) in a quartz tube was heated with a temperature ramp-rate of $10^\circ\text{C min}^{-1}$ in a flow of 5% H_2/Ar ($20\text{ cm}^3\text{ min}^{-1}$). The effluent gas was passed through a trap containing MS4 Å to remove water, then through the thermal conductivity detector, which detected the amount of H_2 consumed during the experiment. The number of surface Pt^0 atoms on Pt/C, pre-reduced in H_2 at 300°C for 0.5 h, was estimated from the CO uptake of the samples at room temperature using the pulse-adsorption of CO in a flow of He by BELCAT (MicrotracBEL). The average Pt particle size was calculated from the CO uptake assuming that CO was adsorbed on the surface of spherical Pt particles at a stoichiometry of $\text{CO}/(\text{surface Pt atom}) = 1/1$. Transmission electron microscopy (TEM) observation of Pt/C was carried out by a JEOL JEM-2100 F TEM operated at 200 kV.

2.3. Catalytic tests

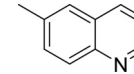
Typically, 5 wt% Pt/C was used as the standard catalyst. After the H_2 -reduction of the catalyst at 300°C , catalytic tests were carried out using a batch-type reactor without exposing the catalyst to air as follows. A mixture of 6-methyl 1,2,3,4-tetrahydroquinoline (1.0 mmol) and *n*-dodecane (0.29 mmol) in *o*-xylene (1.5 mL) was injected to the pre-reduced catalyst inside the reactor (cylindrical glass tube) through a septum inlet, followed by filling N_2 . Then, the resulting mixture in a 15 mL of closed reflux system under 1 atm N_2 was magnetically stirred and was heated to reflux temperature; the bath temperature was 160°C and reaction temperature was *ca.* 144°C . The yield of 6-methyl-quinoline was determined by GC (Shimadzu GC-14 B with Ultra ALLOY capillary column UA⁺-1 of Frontier Laboratories Ltd., N_2) using *n*-dodecane as an internal standard. Typically, the error in the yield determined by GC was $\pm 1.5\%$. To determine the isolated yield of 6-methyl-quinoline, 6-methyl-quinoline was isolated by column chromatography using silica gel 60 (spherical, 63–210 µm, Kanto Chemical Co. Ltd.) with hexane/ethylacetate (90/10) as the eluting solvent, followed by analyses by GC-MS and ^1H and ^{13}C NMR. The hydrogenation of quinoline was carried out by a stainless autoclave (28 cm^3) at 160°C under 3 bar H_2 .

2.4. NMR and GC-MS analysis

^1H and ^{13}C NMR spectra were recorded at ambient temperature by JEOL-ECX 600 operating at 600.17 and 150.92 MHz, respectively

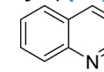
with tetramethylsilane as an internal standard. All chemical shifts (δ) are reported in ppm and coupling constants (J) in Hz. All chemical shifts are reported relative to tetramethylsilane and *d*-solvent peaks (77.00 ppm, chloroform), respectively. Abbreviations used in the NMR experiments: s, singlet d, doublet; t, triplet; m, multiplet. GC-MS spectra were recorded by SHIMADZU QP2010.

2.4.1. 6-Methyl-quinoline (Table 3, entry 1) [18]



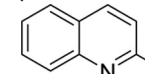
^1H NMR (600.17 MHz, CDCl_3), TMS: δ 8.51 (d, $J = 2.70\text{ Hz}$, 1H), 7.73 (d, $J = 8.94\text{ Hz}$, 1H), 7.54 (d, $J = 7.56\text{ Hz}$, 1H), 7.12 (d, $J = 8.22\text{ Hz}$, 1H), 7.05 (s, 1H), 6.98–6.87 (m, 1H), 2.09 (s, 3H); ^{13}C NMR (150.91 MHz, CDCl_3) δ 148.63, 146.11, 135.36, 134.39, 130.82, 128.27, 127.44, 125.79, 120.17, 20.66; MS m/e 143.07.

2.4.2. Quinoline (Table 3, entry 2) [16]



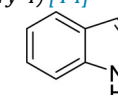
^1H NMR (600.17 MHz, CDCl_3), TMS: δ 8.89 (d, $J = 2.76\text{ Hz}$, 1H), 8.12–8.07 (m, 2H), 7.76 (d, $J = 8.22\text{ Hz}$, 1H), 7.68 (t, $J = 7.56\text{ Hz}$, 1H), 7.50 (t, $J = 7.56\text{ Hz}$, 1H), 7.33–7.32 (m, 1H); ^{13}C NMR (150.91 MHz, CDCl_3) δ 150.15, 148.02, 135.81, 129.22, 129.19, 128.03, 127.57, 126.30, 120.83; MS m/e 129.04.

2.4.3. 2-Methyl-quinoline (Table 3, entry 3) [23]



^1H NMR (600.17 MHz, CDCl_3), TMS: δ 8.03 (d, $J = 8.28\text{ Hz}$, 1H), 7.80 (d, $J = 8.28\text{ Hz}$, 1H), 7.59 (d, $J = 7.56\text{ Hz}$, 2H), 7.34 (t, $J = 6.90\text{ Hz}$, 1H), 7.05 (t, $J = 6.18\text{ Hz}$, 1H), 2.64 (s, 3H); ^{13}C NMR (150.91 MHz, CDCl_3) δ 158.13, 147.18, 135.35, 128.68, 127.95, 126.82, 125.77, 124.93, 121.22, 24.65; MS m/e 143.07.

2.4.4. Indole (Table 3, entry 4) [14]



^1H NMR (600.17 MHz, CDCl_3), TMS: δ 8.09 (s, NH, 1H), 7.65 (d, $J = 8.28\text{ Hz}$, 1H), 7.38 (d, $J = 8.28\text{ Hz}$, 1H), 7.19 (m, 2H), 7.12 (t, $J = 7.20\text{ Hz}$, 1H), 6.55 (s, 1H); ^{13}C NMR (150.91 MHz, CDCl_3) δ 135.74, 127.82, 124.10, 121.96, 120.71, 119.79, 111.00, 102.60; MS m/e 117.10.

3. Result and discussion

3.1. Catalyst characterization

Fig. 1 shows temperature programmed H_2 -reduction ($\text{H}_2\text{-TPR}$) profile of $\text{Pt}(\text{NH}_3)_2(\text{NO}_3)_2$ -loaded carbon as the precursor of Pt/C. The $\text{H}_2\text{-TPR}$ profile shows H_2 consumption peaks below 250°C assignable to the reduction of Pt(II) to metallic Pt. This indicates that the standard Pt/C catalyst pre-reduced at 300°C contains metallic Pt. Fig. 2 shows a representative TEM image and Pt size distribution of Pt/C. The average diameter of Pt particles for 98 particles was $2.9 \pm 0.8\text{ nm}$, and the volume-area mean diameter of Pt particles was $3.5 \pm 0.8\text{ nm}$. The volume-area mean diameter (TEM analysis) was consistent with the mean diameter estimated by the CO adsorption experiment (3.2 nm) within the experimental error of TEM analysis, which supported the TEM results. Summarizing the above characterization results, we conclude that Pt species in the standard Pt/C catalyst are present as 3.5 nm sized Pt metal nanoparticles.

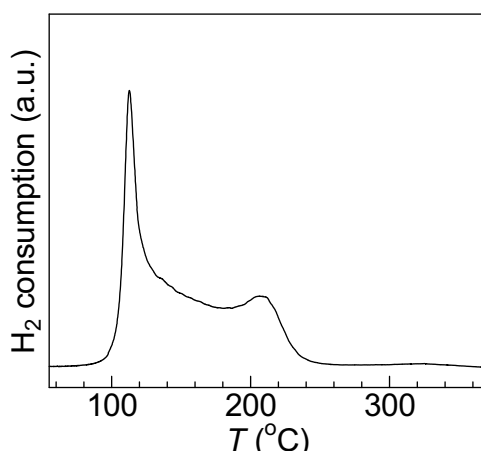


Fig. 1. H₂-TPR profile of Pt(NH₃)₂(NO₃)₂-loaded carbon.

3.2. Catalytic tests

In order to optimize catalyst compositions and reaction conditions, we carried out dehydrogenation of 6-methyl-1,2,3,4-tetrahydroquinoline (**1a**) into 6-methyl-quinoline (**1b**) under refluxing of *o*-xylene in 1 atm N₂ for 6 h in the presence of 1 mol% of Pt. **Table 1** shows the results of the Pt catalysts on various supports pre-reduced at 300 °C. Among the catalysts tested, Pt/C (entry 1) showed the highest yield (81%). Pt/SiO₂ and Pt/HBEA (entries 4,5) showed 25% yields, and Pt/Al₂O₃, Pt/MgO, Pt/TiO₂, Pt/Nb₂O₅, Pt/ZrO₂ and Pt/SnO₂ gave low yields of 6–19%. The platinum oxides-loaded carbon (PtOx/C) catalyst showed no activity (entry 3). When the pre-reduced Pt/C was exposed to air at room temperature for 0.5 h, the air-exposed catalyst (Pt/C-air in entry 2) showed lower yield (58%) than the as-reduced Pt/C catalyst (81%) possibly due to the oxidation of some of the surface Pt⁰ species. These results indicates that metallic Pt⁰ is the active species in this catalytic system.

Table 1
Dehydrogenation of **1a** by supported Pt catalysts reduced at 300 °C.

1a 1 mmol	Pt/support (0.01 mmol Pt) 1.5 mL <i>o</i> -xylene, reflux under N ₂ , 6 h	1b
Entry	Catalyst	Yield(%)
1	Pt/C	81
2	Pt/C-air	58
3	PtOx/C	0
4	Pt/SiO ₂	25
5	Pt/HBEA	25
6	Pt/SiO ₂ -Al ₂ O ₃	19
7	Pt/Al ₂ O ₃	19
8	Pt/MgO	18
9	Pt/TiO ₂	12
10	Pt/Nb ₂ O ₅	16
11	Pt/ZrO ₂	9
12	Pt/SnO ₂	6

a PtOx/C was not reduced before the reaction.

Adopting carbon as the most effective support material, we next screened various metal-loaded carbon (M/C) catalysts for the model dehydrogenation of **1a** (1 mmol) using only 0.1 mol% (0.001 mmol) of active metals (Pt, Ir, Ag, Pd, Rh, Ru, Cu, Ni, Co). **Table 2** lists the yield of **1b** for the catalysts in the initial period of the reaction (6 h). The yields changed in the order of Co/C < Ag/C < Cu/C < Ni/C < Ru/C < Ir/C < Pd/C < Rh/C < Pt/C. **Fig. 3** (left) compares the time course of the reaction for representative catalysts. Among the catalysts, Pt/C catalyst showed the highest activity in terms of the initial rate and the final yield (96%) after 50 h. The final yields for Ir/C (83%), Pd/C (72%) and Ru/C (70%) were moderately high, while the other catalysts showed low yields (<40%) after 50 h. For the standard Pt/C catalyst, the time course profile in **Fig. 3** (right) shows that the conversions of **1a** and the yields of **1b** were nearly close to each other during the reaction, which indicates that **1a** is selectively transformed to **1b**.

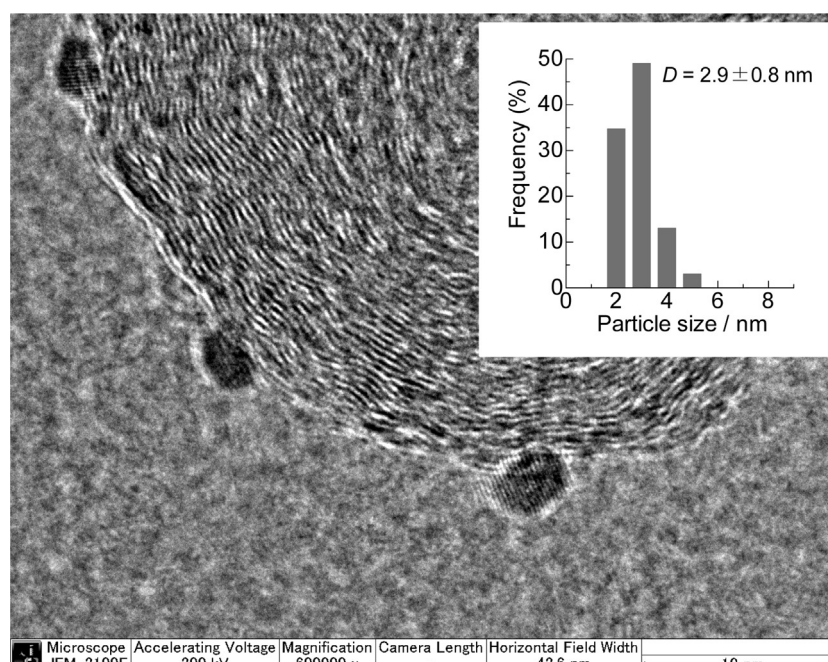


Fig. 2. A representative TEM image and Pt particle size distribution of Pt/C (pre-reduced at 300 °C). The mean diameter of Pt particle was 2.9 ± 0.8 nm, and the volume-area mean diameter was 3.5 ± 0.8 nm.

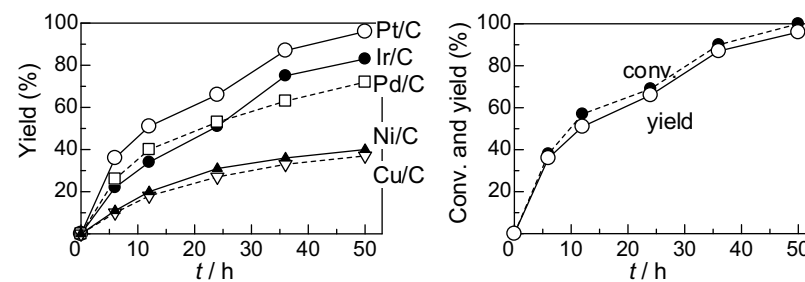


Fig. 3. Time-yield profiles for various metal-loaded carbon catalysts (left) and time course of the reaction for the standard Pt/C catalyst (right). Conditions are shown in Table 2.

Table 2

Dehydrogenation of **1a** by carbon-supported metal catalysts reduced at 300 °C.

1a		metal/C (0.1 mol%)	1b
1 mmol		1.5 mL <i>o</i> -xylene, reflux under N ₂ , 6 h	+ 2H ₂
1	Pt/C	36	
2	Rh/C	28	
3	Pd/C	26	
4	Ir/C	22	
5	Ru/C	17	
6	Ni/C	11 (7) ^a	
7	Cu/C	10	
8	Ag/C	6	
9	Co/C	5 (7) ^a	

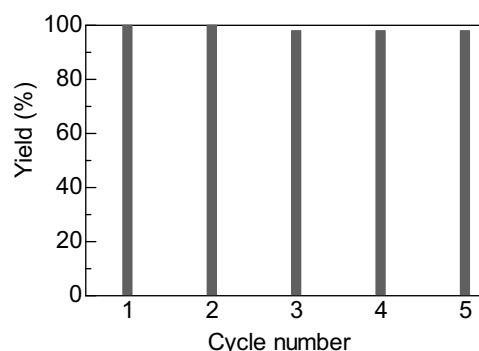


Fig. 4. Catalyst reuse for dehydrogenation of **1a** (1 mmol) under N₂ in refluxing *o*-xylene (1.5 mL) for 11 h using Pt/C (1 mol% Pt with respect to **1a**).

Fig. 4 shows the results of catalyst reusability of Pt/C for the dehydrogenation of **1a**. After the first cycle, 2-propanol (1 mL) was added to the reaction mixture and the catalyst was separated by centrifugation. Then, 6-methyl-quinoline (**1b**) in the solution was isolated by column chromatography. The yield of the isolated 6-methyl-quinoline (94%) was close to the yield determined by GC (98%). The separated Pt/C catalyst was washed with acetone three times, followed by centrifugation and drying in oven (under air) at 90 °C for 12 h and by reduction in H₂ at 300 °C for 0.5 h. After the treatment, the recovered Pt/C catalyst showed 96–98% GC yields of **1b** during the next four recycle tests. In a separate experiment, ICP-AES analysis of the filtrate after the first reaction with Pt/C showed that the content of Pt in the solution was 0.35 ppm, corresponding to 0.024% of Pt in the catalyst used.

Table 3 shows the substrate scope for dehydrogenation of various *N*-heterocycles (1 mmol) in the presence of 0.1 mol% (0.001 mmol) of Pt/C. Derivatives of tetrahydroquinoline, including 6-methyl-1,2,3,4-tetrahydroquinoline

Table 3

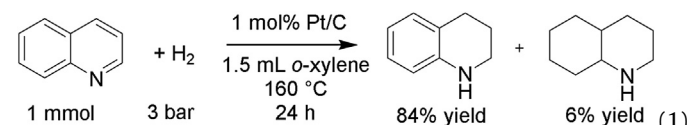
Dehydrogenation of saturated *N*-heterocycles by Pt/C^a.

Entry	Substrate	Product	t (h)	Conv. (%)	Yield (%)
1			50	100	96
2			65	100	91
3			60	100	93
4			45	100	97

b Conditions: 1 mmol *N*-heterocycles in 1.5 mL *o*-xylene, reflux, 0.1 mol% Pt/C

(entry 1), 1,2,3,4-tetrahydroquinoline (entry 2) and 2-methyl-1,2,3,4-tetrahydroquinoline (entry 3) were transformed to 6-methyl-quinoline, quinoline and 2-methyl-quinoline, respectively, with high yields (91–96%). Indoline (entry 4) was also converted to indole with high yield (97%). For the dehydrogenation of 1,2,3,4-tetrahydroquinoline (entry 2), 91% yield of quinoline corresponds to TON of 910, which is higher than those of the previous homogeneous [4,7,8,6,9] and heterogeneous [2,3] catalysts (TON = 3.3–87). These results show that the method is effective for the oxidant-free dehydrogenation of various *N*-heterocycles.

Under 3 bar H₂, the same catalytic system was effective for hydrogenation of quinoline. As shown in Eq. (1), the hydrogenation reaction of quinoline by 1 mol% of the Pt/C catalyst under 3 bar H₂ in an autoclave reactor at 160 °C gave 1,2,3,4-tetrahydroquinoline in 84% yield together with 6% yield of *trans*-decahydroquinoline as an undesirable side product.



Finally, we study the relationship between the electronic properties of various metals and the catalytic activity of various metals loaded on carbon for the dehydrogenation of **1a** and discuss a possible reason why Pt/C gave higher activity than the other metals (Table 2). Fig. 5 plots the initial rate of the dehydrogenation (from Table 2 [24]) as a function of the d-band center (ε_d) relative to the Fermi energy (E_F), $\varepsilon_d - E_F$, for the clean metal surface calculated by Hammer and Nørskov using DFT method [25]. The d-band center has been used as a descriptor of activity trends in various transition metal surfaces [25–27]. The result in Fig. 5 shows a typical volcano-

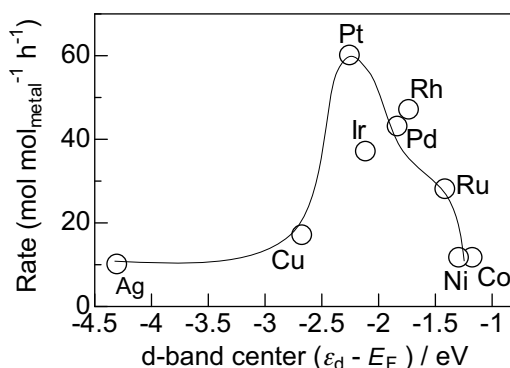


Fig. 5. Effect of the d-band center of the metals relative to the Fermi energy [25] on the initial rate of **1b** formation for dehydrogenation of **1a** by carbon-supported metal catalysts (from Table 2).

type dependence of the catalytic activity on the d-band center; the platinum-group-metals (Pt, Ir, Pd, Rh, Ru) having intermediate d-band center show higher catalytic activity than the metals with a deep ε_d levels (Ag, Cu) and the metals with d-band centers close to E_F (Ni, Co). Taking into account a general tendency that the bond strength between a metal surface (M) and a hydrogen atom (H) is weaker for a metal with deeper ε_d level [26] and that the catalytic dehydrogenation of *N*-heterocycles can include the formation and dissociation of M–H bonds, the result suggests that a moderate M–H bond strength is favorable for this catalytic system. The metals with a deep ε_d levels (Ag, Cu) may show low activity for the C–H dissociation step than platinum-group-metals, while strong M–H bonds on the metals with d-band centers close to E_F (Ni, Co) may show low activity for the M–H dissociation step (H_2 desorption step). Similar volcano-type dependence has been observed for several catalytic systems [26,27].

4. Conclusions

We found that Pt metal nanoparticles-loaded carbon (Pt/C) was effective and reusable heterogeneous catalyst for oxidant-free dehydrogenation of *N*-heterocycles. Derivatives of tetrahydroquinoline and indoline were converted to quinolines and indole with high yields. For the dehydrogenation of 1,2,3,4-tetrahydroquinoline, TON of Pt/C was more than one order of magnitude higher than those of the previous homogeneous and heterogeneous catalysts. Additionally, the same catalyst was effective for the reverse reaction, hydrogenation of quinoline under 3 bar H_2 . Thus,

this catalytic method may be useful for an organic halide-based hydrogen storage system.

Acknowledgment

This work was supported by JSPS KAKENHI (Grant No. 26289299), a MEXT program “Elements Strategy Initiative to Form Core Research Center” and a Grant-in-Aid for Scientific Research on Innovative Areas “Nano Informatics” (25106010) from JSPS.

References

- [1] T. Hara, K. Mori, T. Mizugaki, K. Ebizaki, K. Kaneda, *Tetrahedron Lett.* **44** (2003) 6207–6210.
- [2] Y. Mikami, K. Ebata, T. Mitsudome, T. Mizugaki, K. Jitsukawa, K. Kaneda, *Heterocycles* **82** (2011) 1371–1377.
- [3] D. Damodara, R. Arundhati, P.R. Likhari, *Adv. Synth. Catal.* **356** (2014) 189–198.
- [4] R. Yamaguchi, C. Ikeda, Y. Takahashi, K. Fujita, *J. Am. Chem. Soc.* **131** (2009) 8410–8412.
- [5] K. Fujita, Y. Tanaka, M. Kobayashi, R. Yamaguchi, *J. Am. Chem. Soc.* **136** (2014) 4829–4832.
- [6] R. Xu, S. Chakraborty, H. Yuan, W.D. Jones, *ACS Catal.* **5** (2015) 6350–6354.
- [7] J. Wu, D. Talwar, S. Johnston, M. Yan, J. Xiao, *Angew. Chem. Int. Ed.* **52** (2013) 6983–6987.
- [8] K.T. Tseng, A.M. Rizzi, N.K. Szymczak, *J. Am. Chem. Soc.* **135** (2013) 16352–16355.
- [9] S. Chakraborty, W.W. Brennessel, W.D. Jones, *J. Am. Chem. Soc.* **136** (2014) 8564–8567.
- [10] K. Yamaguchi, N. Mizuno, *Angew. Chem. Int. Ed.* **42** (2003) 1480–1483.
- [11] K. Kamata, J. Kasai, K. Yamaguchi, N. Mizuno, *Org. Lett.* **6** (2004) 3577–3580.
- [12] T. Tanaka, K. Okunaga, M. Hayashi, *Tetrahedron Lett.* **51** (2010) 4633–4635.
- [13] D. Dean, B. Davis, P.G. Jessop, *New J. Chem.* **35** (2011) 417–422.
- [14] S. Venkatesan, A.S. Kumar, J.-F. Lee, T.-S. Chan, J.-M. Zen, *Chem. Eur. J.* **18** (2012) 6147–6151.
- [15] D. Ge, L. Hu, J. Wang, X. Li, F. Qi, J. Lu, X. Cao, H. Gu, *ChemCatChem* **5** (2013) 2183–2186.
- [16] S. Furukawa, A. Suga, T. Komatsu, *Chem. Commun.* **50** (2014) 3277–3280.
- [17] D.V. Jawale, E. Gravel, N. Shah, V. Dauvois, H. Li, I.N.N. Namboothiri, E. Doris, *Chem. Eur. J.* **21** (2015) 7039–7042.
- [18] A.V. Iosub, S.S. Stahl, *Org. Lett.* **17** (2015) 4404–4407.
- [19] S.-I. Murahashi, T. Naota, T.H. Taki, *J. Chem. Soc. Chem. Commun.* (1985) 613–614.
- [20] P. Müller, D.M. Gilabert, *Tetrahedron* **44** (1988) 7171–7175.
- [21] A.E. Wendlandt, S.S. Stahl, *J. Am. Chem. Soc.* **136** (2014) 11910–11913.
- [22] S.K. Moromi, A.S. Touchy, S.M.A.H. Siddiki, M.A. Ali, K. Shimizu, *RSC Adv.* **5** (2015) 1059–1062.
- [23] C.J. Pouchert, J. Behnke (Eds.), *The Aldrich Library of ¹³C and ¹H FT NMR Spectra*, vol. 3, 1st edn., Aldrich Chemical Company Inc., Milwaukee, 1993, p. 421B.
- [24] H₂-TPR showed that the precursors of Ni/C and Co/C catalysts were reduced to metallic states by reduction at 500 °C. The catalytic tests of Ni/C and Co/C catalysts after reduction at 500 °C are shown in parentheses of Table 2, and the results are converted to the reaction rates in Fig. 5.
- [25] B. Hammer, J.K. Norskov, *Adv. Catal.* **45** (2000) 71–129.
- [26] H. Toulhoat, P. Raybaud, *J. Catal.* **216** (2003) 63–72.
- [27] M. Tamura, K. Kenichi, A. Satsuma, K. Shimizu, *ACS Catal.* **2** (2012) 1904–1909.